

Communication

# Towards Li-Ion Batteries Operating at 80 °C: Ionic Liquid versus Conventional Liquid Electrolytes

Gabriel Oltean <sup>1</sup>, Nareerat Plylahan <sup>2</sup>, Charlotte Ihrfors <sup>1</sup>, Wei Wei <sup>1</sup>, Chao Xu <sup>1</sup> , Kristina Edström <sup>1</sup>, Leif Nyholm <sup>1</sup> , Patrik Johansson <sup>2</sup> and Torbjörn Gustafsson <sup>1,\*</sup>

<sup>1</sup> Department of Chemistry—Ångström Laboratory, Uppsala University, Box 538, Uppsala SE-75121, Sweden; gabriel.oltean@scania.com (G.O.); charlotte.ihrfors@kemi.uu.se (C.I.); wwei815@gmail.com (W.W.); chao.xu@kemi.uu.se (C.X.); Kristina.Edstrom@kemi.uu.se (K.E.); leif.nyholm@kemi.uu.se (L.N.)

<sup>2</sup> Department of Physics, Chalmers University of Technology, Göteborg SE-41296, Sweden; nareerat.plylahan@volvo.com (N.P.); patrik.johansson@chalmers.se (P.J.)

\* Correspondence: torbjorn.gustafsson@kemi.uu.se; Tel.: +46-(0)18-471-3766

Received: 19 October 2017; Accepted: 24 November 2017; Published: 2 January 2018

**Abstract:** Li-ion battery (LIB) full cells comprised of TiO<sub>2</sub>-nanotube (TiO<sub>2</sub>-nt) and LiFePO<sub>4</sub> (LFP) electrodes and either a conventional organic solvent based liquid electrolyte or an ionic liquid based electrolyte have been cycled at 80 °C. While the cell containing the ionic liquid based electrolyte exhibited good capacity retention and rate capability during 100 cycles, rapid capacity fading was found for the corresponding cell with the organic electrolyte. Results obtained for TiO<sub>2</sub>-nt and LFP half-cells indicate an oxidative degradation of the organic electrolyte at 80 °C. In all, ionic liquid based electrolytes can be used to significantly improve the performance of LIBs operating at 80 °C.

**Keywords:** Li-ion batteries; ionic liquid; elevated temperature

## 1. Introduction

Due to their high energy and power densities, state-of-the-art Li-ion batteries (LIBs) are widely used for portable electronics, as well as for electric and hybrid electric vehicles. The key issues to address to ensure a continuous increase in the use of LIBs for large scale electrical energy storage are safety [1] and sustainability [2]. Since high operating or storage temperatures (i.e., above 50 °C) can give rise to significant fading for most commercial LIBs [3,4], cooling systems are generally required. With LIBs working at elevated temperatures—e.g., between 80 and 100 °C—the thermal management in a hybrid electric vehicle could be significantly simplified by allowing the cooling system for the power electronics to also take care of the cooling of the battery pack, resulting in a significant reduction in the complexity and price [5].

The Li polymer battery employed by Bolloré in Autolib' vehicles represents an example of a successful battery operating at about 80 °C [6]. However, in the scientific literature the term “high temperature cycling” mainly refers to cycling at temperatures at 60 or 70 °C, with only a few reports of battery cycling at 80 °C or higher [7–20]. The majority of these studies have been carried out with organic carbonate based electrolytes [7–15], but ionic liquid (IL) based electrolytes [16–18], solid polymer electrolytes [19], and ternary electrolytes (IL + polymer + Li-salt) [20] have also been explored. The extensive work with traditional carbonate electrolytes has aimed at finding suitable electrolyte additives [7], alternative binders [8], and the failure mechanisms for both the negative [9,10] and positive electrodes [11–13] as well as full cells [14,15]. Unfortunately, so far there are no promising results for these electrolytes when cycling at temperatures of 80 °C or above.

Work with IL-based electrolytes has, on the other hand, demonstrated promising cycling stabilities for titanium dioxide, TiO<sub>2</sub>(B), and LiFePO<sub>4</sub> (LFP) half-cells at temperatures as high as 120 °C [16–18]. The cycling of LIBs at elevated temperatures such as 80 °C is associated with increased risks as

the kinetics of any side reaction are enhanced, which could lead to the initiation of heat-generating exothermic reactions and eventually thermal runaway [21]. The safety of LIBs operating at these temperatures can therefore be significantly improved if more stable IL electrolytes were used. Pyrrolidinium (Pyr) based ILs have been shown to have wide electrochemical stability windows [16,22]. Moreover,  $\text{TiO}_2$  electrodes can be cycled at temperatures as high as 120 °C with an electrolyte composed of 1 M lithium bis(trifluoromethanesulfonyl)imide (LiTFSI) in *N*-methyl-*N*-propylpyrrolidinium TFSI (Pyr13TFSI) [16]. It should be mentioned that the previous studies [16–18] were carried out in half-cell configurations with Li metal as the anode material. The electrochemical performance of ionic liquid electrolytes at elevated temperature should therefore also be investigated in full cell Li-ion batteries.

In the present work, LIB cells containing  $\text{TiO}_2$  nanotube ( $\text{TiO}_2\text{-nt}$ ) negative electrodes and LFP positive electrodes are cycled at 80 °C using two different electrolytes: 1 M LiTFSI in propylene carbonate (PC), as an example of a conventional organic solvent based electrolyte, and an IL based electrolyte composed of LiTFSI in Pyr13TFSI (i.e.,  $\text{Li}_{0.2}\text{Pyr13}_{0.8}\text{TFSI}$ ).  $\text{TiO}_2$  was chosen as the negative electrode material due to its high redox potential (ca. 1.78 V vs.  $\text{Li}^+/\text{Li}$  [23]), which should result in insignificant formation of any solid electrolyte interphase (SEI) layer. In addition, LFP is known to be a safe material with a high thermal stability [24]. The electrochemical behavior of the cells during 100 cycles is investigated and discussed with special focus on the failing mechanism of the cells containing the conventional organic electrolyte.

## 2. Results and Discussion

The electrochemical performance of the  $\text{TiO}_2\text{-nt}$  half-cell containing the organic electrolyte indicated a 10% irreversible capacity loss on the first discharge, and a capacity of about 148 mAh/g after 100 cycles (Figure 1a,b). As the capacity decrease was only 5% between the 2nd and the 100th cycle, it is clear that the main decrease took place between the 1st and the 2nd cycles. The coulombic efficiency for the  $\text{TiO}_2\text{-nt}$  half-cell was 88.5% on the first cycle, indicating that not all lithium could be extracted from the  $\text{TiO}_2\text{-nt}$  electrode upon charge. As the electrode already contained some lithium prior to the second cycle lithiation, the discharge plateau was situated at a slightly higher potential, i.e., the lithiation overpotential was lower. Nevertheless, the coulombic efficiency increased to 98.7% on the second cycle and subsequently stabilized at 99.7% (Figure 1b). These results indicate that the  $\text{TiO}_2\text{-nt}$  electrodes readily can be used at 80 °C.

A continuous capacity decrease was, however, observed during the cycling of the LFP based half-cell (Figure 1c,d). The results also indicate the presence of an irreversible oxidation reaction most likely involving the electrolyte, as the charge capacity always was larger than the discharge capacity (Figure 1c). Since the coulombic efficiency decreased dramatically during the first five cycles, only to slowly increase again upon further cycling, it is reasonable to assume that a layer of electrolyte degradation products was formed on the electrode surface mainly during the first five cycles. This behavior is in stark contrast to that seen for LFP electrodes cycled at room temperature, in which case stable cycling and high coulombic efficiency are typically observed [25]. The continuous capacity loss upon cycling, leading to a capacity loss of 25% after 100 cycles is clearly detrimental to the performance of any full cell and thus conventional organic solvent based electrolytes are less suitable for LIBs operated at 80 °C.

The  $\text{TiO}_2\text{-nt}$  and LFP half-cells were also subject to rate capability tests (Figure 2). For the  $\text{TiO}_2\text{-nt}$  half-cell, the capacity was found to decrease with increasing rate but there was no significant permanent loss of capacity during the cycling, i.e., the same capacity was obtained when the rate was decreased to C/5 again. This behavior can therefore be explained by the increased iR drop at higher cycling rates. The corresponding results for the LFP half-cell (Figure 2b), on the other hand, features a significant capacity decrease upon cycling irrespective of the cycling rate employed which is in good agreement with the poor cycling stability (Figure 1c,d).

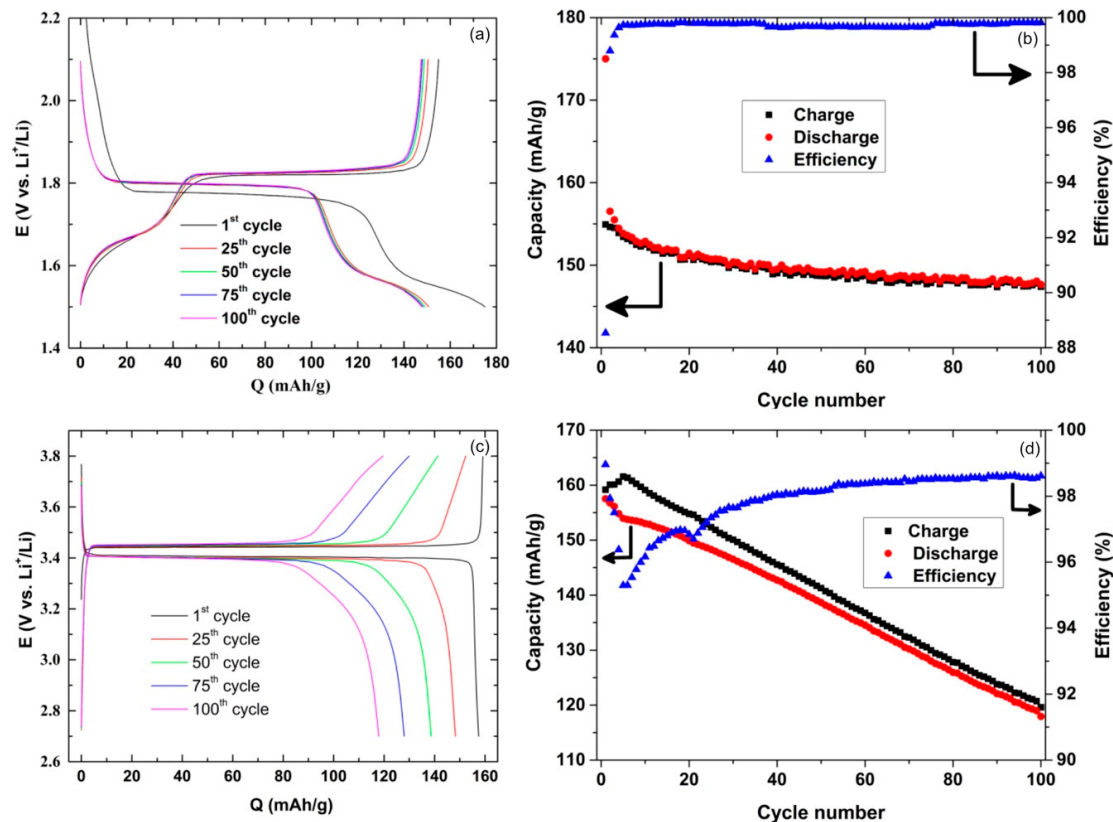


**Figure 1.** Charge and discharge curves (a,c), and the capacity and coulombic efficiency as a function of the cycle number (b,d) for a  $\text{TiO}_2\text{-nt}$  half-cell (a,b) and a LFP half-cell (c,d). The rate was C/5 at 80  $^{\circ}\text{C}$  using a 1 M LiTFSI in PC electrolyte.

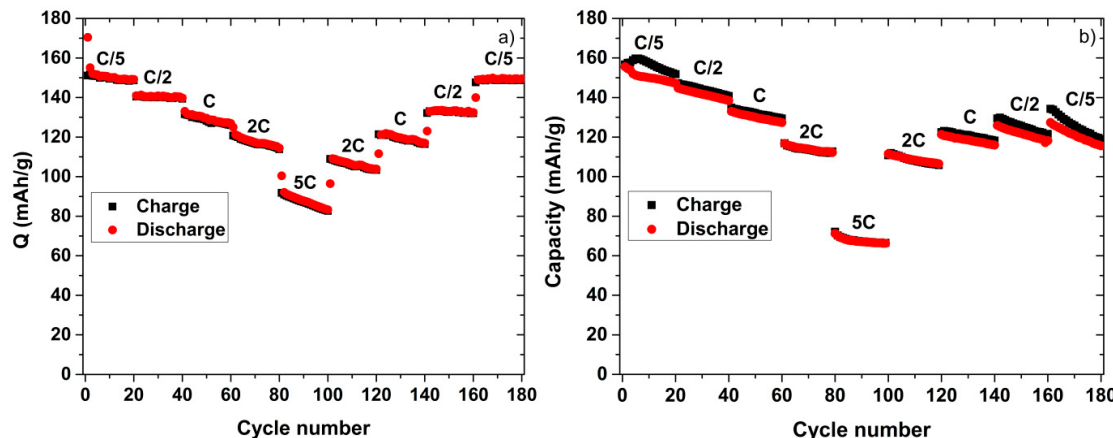


**Figure 2.** Rate capabilities for the  $\text{TiO}_2\text{-nt}$  (a) and LFP (b) based half-cells at 80  $^{\circ}\text{C}$  using a 1 M LiTFSI in PC electrolyte.

Cycling of full cells containing a  $\text{TiO}_2\text{-nt}$  negative electrode and a LFP positive electrode using the two different electrolytes was also carried out (Figure 3). During 100 cycles, there was almost no capacity fading for the cell containing the IL based electrolyte (Figure 3a), while a significant loss of capacity was obtained for the cell containing the organic electrolyte (insert). This clearly shows that the IL based electrolyte is more stable towards oxidation compared to the conventional organic electrolyte. The capacity obtained at a rate of 2C was about 65% of that found at a rate of C/5 (~110 mAh/g) (Figure 3b). In analogy with the results for the  $\text{TiO}_2\text{-nt}$  half-cell this suggests a loss of capacity at the higher rates mainly due to iR drop effects.

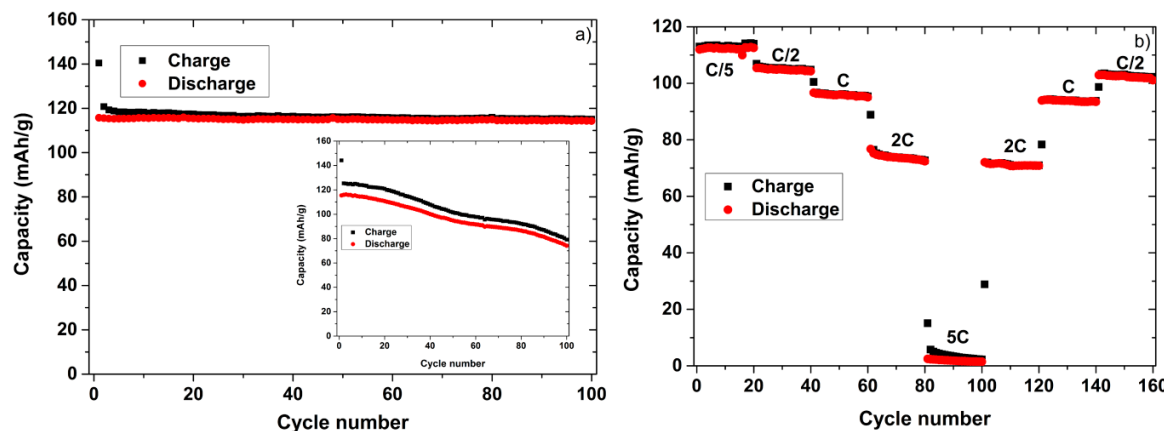


**Figure 3.** The C/5 capacity as a function of the cycle number (a) and the rate capability (b) obtained at 80 °C for a full cell containing a TiO<sub>2</sub>-nt negative electrode, a LFP positive electrode, and a Li<sub>0.2</sub>Pyr13<sub>0.8</sub>TFSI electrolyte. The inset in (a) shows the corresponding full cell data obtained for the 1 M LiTFSI in PC electrolyte.

### 3. Materials and Methods

The TiO<sub>2</sub>-nt electrodes were fabricated using a previously described two-step anodization process [26]. The first anodization step was carried out by stepping the potential from 0 to 60 V after which this potential was maintained for around four hours. The obtained nanotube layer was then removed by strong sonication in deionized water (DI) for 20 min to expose the underlying titanium substrate. The second anodization was then performed on this textured substrate for 90 min using the same experimental conditions, after which the sample was rinsed in DI and dried in a flow of nitrogen. The TiO<sub>2</sub>-nt electrodes were subsequently thermally annealed in air at 350 °C for five hours. The LFP electrodes were obtained by casting a slurry containing 75 wt % LiFePO<sub>4</sub> (Phostech, P2), 15 wt % PVdF (Solvay, Solef 5130), and 10 wt % conductive carbon (Timcal, Super C 65) on aluminum foil. All electrodes were dried in vacuum at 120 °C for 12 h prior to use in the LIB cells.

The organic carbonate based electrolyte was made by dissolving LiTFSI (99.95%) in PC (BASF, >99.8%) to a concentration of 1 M. The IL electrolyte was prepared by mixing LiTFSI with Pyr13TFSI (99%) to yield a mole fraction of 0.2 i.e., Li<sub>0.2</sub>Pyr13<sub>0.8</sub>TFSI.

The LIB full cells contained a TiO<sub>2</sub>-nt negative electrode separated from the LFP positive electrode by a glass fiber separator impregnated with the selected electrolyte, all vacuum sealed in a polymer coated aluminum pouch cell. The half-cells consisted of a TiO<sub>2</sub>-nt or LFP working electrode and a lithium foil serving as a combined counter and reference electrode, separated by a glass fiber separator impregnated with the organic electrolyte. All cells were galvanostatically tested at 80 °C using a Digatron BTS600 galvanostat and the TiO<sub>2</sub>-nt half-cells were cycled between 1.5 and 2.1 V vs. Li<sup>+</sup>/Li° whereas the LFP half-cells were cycled between 2.7 and 3.8 V vs. Li<sup>+</sup>/Li°. The TiO<sub>2</sub>-nt-LFP full-cells were cycled between 1.4 and 2.1 V.

### 4. Conclusions

The electrochemical cycling performance of cells composed of TiO<sub>2</sub>-nt negative electrodes and LFP positive electrodes at 80 °C critically depends on the choice of the electrolyte. While cells containing a Li<sub>0.2</sub>Pyr13<sub>0.8</sub>TFSI ionic liquid electrolyte could be cycled without significant loss of capacity for 100 cycles at 80 °C, significant capacity decays were found with a conventional organic liquid electrolyte. The latter was attributed to an oxidative degradation of the organic electrolyte, yielding low coulombic efficiencies. The excellent performance of the ionic liquid based full cells seen for rates up to 2C provide new possibilities for the development of safe, stable, and sustainable LIBs for use at elevated temperatures in, e.g., hybrid electric heavy vehicles.

**Acknowledgments:** “High Temperature Lithium-ion Batteries” is a project funded by the Swedish Energy Agency via “Batterifonden” and the collaboration between Chalmers University of Technology, Lund University, Uppsala University, and Scania CV AB was created within the Swedish Electromobility Center (SHC). The Swedish Strategic Research Foundation and the project “Road to Load” (a collaboration between Uppsala University and Chalmers University of Technology) are also acknowledged.

**Author Contributions:** G.O., K.E., L.N., P.J., and T.G. conceived and designed the experiments. G.O., N.P., and C.I. executed the experiments. C.I. and P.J. provided the ionic liquid. C.I. and W.W. provided the  $\text{TiO}_2$ -nt electrodes. G.O., T.G., L.N., C.I., and W.W. were involved in the analysis of the results. G.O. and C.X. wrote the manuscript. All authors were involved in the discussion of the results and manuscript.

**Conflicts of Interest:** The authors declare no conflict of interest.

## References

1. Kalhoff, J.; Eshetu, G.G.; Bresser, D.; Passerini, S. Safer Electrolytes for Lithium-Ion Batteries: State of the Art and Perspectives. *ChemSusChem* **2015**, *8*, 2154–2175. [CrossRef] [PubMed]
2. Larcher, D.; Tarascon, J.-M. Towards greener and more sustainable batteries for electrical energy storage. *Nat. Chem.* **2015**, *7*, 19–29. [CrossRef] [PubMed]
3. Bloom, I.; Cole, B.W.; Sohn, J.J.; Jones, S.A.; Polzin, E.G.; Battaglia, V.S.; Henriksen, G.L.; Motloch, C.; Richardson, R.; Unkelhaeuser, T.; et al. An accelerated calendar and cycle life study of Li-ion cells. *J. Power Sources* **2001**, *101*, 238–247. [CrossRef]
4. Vetter, J.; Novák, P.; Wagner, M.; Veit, C.; Möller, K.-C.; Besenhard, J.; Winter, M.; Wohlfahrt-Mehrens, M.; Vogler, C.; Hammouche, A. Ageing mechanisms in lithium-ion batteries. *J. Power Sources* **2005**, *147*, 269–281. [CrossRef]
5. Tidblad, A.; Svens, A.P. Energirelaterad Fordonsforskning 2017. Available online: <https://www.energimyndigheten.se/globalassets/forskning--innovation/konferenser/energirelaterad-fordonsforskning/program-energirelaterad-fordonsforskning-2017.pdf> (accessed on 29 December 2017).
6. Vervaeke, M.; Calabrese, G. Prospective design in the automotive sector and the trajectory of the Bluecar project: An electric car sharing system. *Int. J. Veh. Des.* **2015**, *68*, 245–264. [CrossRef]
7. Smart, M.C.; Ratnakumar, B.V.; Gozdz, A.S.; Mani, S. The Effect of Electrolyte Additives upon the Lithium Kinetics of Li-Ion Cells Containing MCMB and  $\text{LiNi}_{x}\text{Co}_{1-x}\text{O}_2$  Electrodes and Exposed to High Temperatures. *ECS Trans.* **2010**, *25*, 37–48. [CrossRef]
8. Morishita, M.; Mukai, T.; Sakamoto, T.; Yanagida, M.; Sakai, T. Improvement of Cycling Stability at 80 °C for 4 V-Class Lithium-Ion Batteries and Safety Evaluation. *J. Electrochem. Soc.* **2013**, *160*, A1311–A1318. [CrossRef]
9. Andersson, A.M.; Edström, K. Chemical composition and morphology of the elevated temperature SEI on Graphite. *J. Electrochem. Soc.* **2001**, *148*, A1100–A1109. [CrossRef]
10. Markevich, E.; Pollak, E.; Salitra, G.; Aurbach, D. On the performance of graphitized meso carbon microbeads (MCMB)–meso carbon fibers (MCF) and synthetic graphite electrodes at elevated temperatures. *J. Power Sources* **2007**, *174*, 1263–1269. [CrossRef]
11. Muto, S.; Sasano, Y.; Tatsumi, K.; Sasaki, T.; Horibuchi, K.; Takeuchi, Y.; Ukyo, Y. Capacity-fading mechanisms of  $\text{LiNiO}_2$ -based lithium-ion batteries II. Diagnostic analysis by electron microscopy and spectroscopy. *J. Electrochem. Soc.* **2009**, *156*, A371–A377. [CrossRef]
12. Sun, Y.-K. Structural degradation mechanism of oxysulfide spinel  $\text{LiAl}_{0.24}\text{Mn}_{1.76}\text{O}_{3.98}\text{S}_{0.02}$  cathode materials on high temperature cycling. *Electrochem. Commun.* **2001**, *3*, 199–202. [CrossRef]
13. Yabuuchi, N.; Ohzuku, T. Electrochemical behaviors of  $\text{LiCo}_{1/3}\text{Ni}_{1/3}\text{Mn}_{1/3}\text{O}_2$  in lithium batteries at elevated temperatures. *J. Power Sources* **2005**, *146*, 636–639. [CrossRef]
14. Bodenes, L.; Dedryvère, R.; Martinez, H.; Fischer, F.; Tessier, C.; Pérès, J.-P. Lithium-ion batteries working at 85 °C: Aging phenomena and electrode/electrolyte interfaces studied by XPS. *J. Electrochem. Soc.* **2012**, *159*, A1739–A1746. [CrossRef]
15. Bodenes, L.; Naturel, R.; Martinez, H.; Dedryvère, R.; Menetrier, M.; Croguennec, L.; Pérès, J.-P.; Tessier, C.; Fischer, F. Lithium secondary batteries working at very high temperature: Capacity fade and understanding of aging mechanisms. *J. Power Sources* **2013**, *236*, 265–275. [CrossRef]

16. Mun, J.; Jung, Y.S.; Yim, T.; Lee, H.Y.; Kim, H.-J.; Kim, Y.G.; Oh, S.M. Electrochemical stability of bis(trifluoromethanesulfonyl) imide-based ionic liquids at elevated temperature as a solvent for a titanium oxide bronze electrode. *J. Power Sources* **2009**, *194*, 1068–1074. [[CrossRef](#)]
17. Matsumoto, H.; Kubota, K. The High Temperature Operation of Lithium Secondary Batteries with Using Ionic Liquids. *ECS Trans.* **2014**, *64*, 425–432. [[CrossRef](#)]
18. Plylahan, N.; Kerner, M.; Lim, D.-H.; Matic, A.; Johansson, P. Ionic liquid and hybrid ionic liquid/organic electrolytes for high temperature lithium-ion battery application. *Electrochim. Acta* **2016**, *216*, 24–34. [[CrossRef](#)]
19. Hu, Q.; Osswald, S.; Daniel, R.; Zhu, Y.; Wesel, S.; Ortiz, L.; Sadoway, D.R. Graft copolymer-based lithium-ion battery for high-temperature operation. *J. Power Sources* **2011**, *196*, 5604–5610. [[CrossRef](#)]
20. Wetjen, M.; Kim, G.-T.; Joost, M.; Winter, M.; Passerini, S. Temperature dependence of electrochemical properties of cross-linked poly(ethylene oxide)-lithium bis(trifluoromethanesulfonyl)imide-N-butyl-N-methylpyrrolidinium bis(trifluoromethanesulfonyl)imide solid polymer electrolytes for lithium batteries. *Electrochim. Acta* **2013**, *87*, 779–787. [[CrossRef](#)]
21. Bandhauer, T.M.; Garimella, S.; Fuller, T.F. A Critical Review of Thermal Issues in Lithium-Ion Batteries. *J. Electrochem. Soc.* **2011**, *158*, R1–R25. [[CrossRef](#)]
22. MacFarlane, D.R.; Meakin, P.; Sun, J.; Amini, N.; Forsyth, M. Pyrrolidinium imides: A new family of molten salts and conductive plastic crystal phases. *J. Phys. Chem. B* **1999**, *103*, 4164–4170. [[CrossRef](#)]
23. Ohzuku, T.; Ohzuku, T. Electrochemistry of anatase titanium dioxide in lithium nonaqueous cells. *J. Power Sources* **1985**, *14*, 153–166. [[CrossRef](#)]
24. Wang, J.; Sun, X. Olivine LiFePO<sub>4</sub>: The remaining challenges for future energy storage. *Energy Environ. Sci.* **2015**, *8*, 1110–1138. [[CrossRef](#)]
25. Delacourt, C.; Poizot, P.; Levasseur, S.; Masquelier, C. Size effects on carbon-free LiFePO<sub>4</sub> powders the key to superior energy density. *Electrochim. Solid State Lett.* **2006**, *9*, A352–A355. [[CrossRef](#)]
26. Wei, W.; Oltean, G.; Tai, C.-W.; Edström, K.; Björefors, F.; Nyholm, L. High energy and power density TiO<sub>2</sub> nanotube electrodes for 3D Li-ion microbatteries. *J. Mater. Chem. A* **2013**, *1*, 8160–8169. [[CrossRef](#)]



© 2018 by the authors. Licensee MDPI, Basel, Switzerland. This article is an open access article distributed under the terms and conditions of the Creative Commons Attribution (CC BY) license (<http://creativecommons.org/licenses/by/4.0/>).